Synthesis and Evaluation of Different Fatty Acid Esters Formulated into Precirol® ATO-Based Lipid Nanoparticles as Vehicles for Topical Delivery

Vanna Sanna,*[,a] Alberto Mariani,[b] Giuseppe Caria,[b] and Mario Sechi[c]

[a] *Prion DGN c/o Porto Conte Research Centre; Fraz. Tramariglio, 07041 Alghero (Sassari), Italy:* [b] *Department of Chemistry and Local INSTM Unit, University of Sassari; and* [c] *Dipartimento Farmaco Chimico Tossicologico, University of Sassari; 07100 Sassari, Italy.* Received January 7, 2009; accepted March 31, 2009; published online April 7, 2009

A series of isopropyl fatty esters having different chain length (C_{13}—C_{23}) were synthesized and formulated in lipid nanoparticles based on Precirol® ATO to evaluate their effect on the physicochemical properties of these latter. Moreover, drug loading and skin permeation of Econazole nitrate, chosen as a lipophilic model drug, were evaluated as well. The obtained nanosystems, prepared by high shear homogenization method, had a mean diameter ranging from 180 to 280 nm and showed an encapsulation efficiency of about 100%. *Ex vivo* permeation results demonstrated a parabolic correlation between permeation effect and chain length of the fatty esters present in the lipid nanoparticles formulated in hydrophilic gels. The maximum flux of drug was observed for the nanoparticles containing esters with 17 and 19 carbon atoms, suggesting that these formulations may constitute a potential carrier for topical delivery of econazole nitrate.

Key words fatty acid ester; lipid nanoparticle; econazole nitrate; skin permeation

Recent progress in nanoparticulate systems have allowed the development of lipid based carriers improving the drug low skin penetration and inducing targeting to specific skin strata.[1—3] In particular, solid lipid nanoparticles (SLN) and nanostructured lipid carriers (NLC) have been proposed as attractive vehicles for controlled release of cosmetic and pharmaceutical substances.[4,5] Both carrier types are submicron size particles (50—1000 nm) and can be distinguished by their inner structure. SLN consist of solid lipids while NLC are formed by a solid matrix entrapping liquid lipid (oil) nanocompartments.[6] These carriers have high affinity toward the stratum corneum (SC) and improve the bioavailability of the encapsulated material to the skin.[7] It is thought that their enhanced skin penetration is primarily due to an increase in skin hydration caused by the occlusive film formed on the skin surface.[8]

The solid lipids most frequently used for the lipid system formulations include triglycerides, partial glycerides, fatty acids and waxes,[9] while the liquid lipids are essentially constituted by oleic acid,[10] and medium chain triglycerides such as caprylic/capric triglycerides.[11]

The use of fatty acids, fatty acid esters and related alcohols as enhancers for drug permeation is of great interest for both topical and transdermal drug delivery.[12,13] Moreover, medium to long chain esters are widely used as ingredients of cosmetics and topical preparations, as they are safer than short chain ones and present the advantage of being one of the endogenous component of human skin lipids.[14] These enhancers decrease the diffusional resistance to permeants by the perturbation of SC lipid bilayers and the creation of "pores" as penetration enhancing effects.[15]

Fatty acid esters differ in several features such as chain length, the presence or absence and the position of possible double bonds, branching schema and substituents. These structural variations can strongly influence their effects as skin penetration enhancers.[16—18]

In our previous work, SLN based on Precirol® ATO (PCR) was developed as carrier for econazole nitrate (ECN) and the behaviors of drug release *in vitro* and *in vivo* were studied.[19]

In this context, we considered of interest to investigate the formulation of various fatty acid esters into nanoparticulate systems and evaluate the influence of the chain length on the permeation enhancement ability.

In general, medium to long chain fatty acids are obtained from many animal and plant sources or by chemical methods, while their isopropyl esters are synthetically prepared, and only a few of them are commercially available. Therefore, we first planned a general and convenient synthetic method in order to prepare a set of isopropyl fatty esters having different chain length (C_{13}—C_{23}, I—VI, Chart 1) by using the corresponding easily available and cheaper fatty acids and isopropyl alcohol as starting materials that were allowed to react in mild conditions.

The obtained fatty esters were then formulated into PCR-based lipid nanoparticles (NLC and SLN) by high shear homogenization method and characterized in terms of particle size, encapsulation efficiency and crystalline structure. As far as the topical administration is concerned, nanoparticles were incorporated into hydrogels, and the *ex vivo* skin permeation of ECN, chosen as a model drug, through porcine SC was evaluated.

Experimental

Materials Econazole Nitrate (ECN) was kindly provided by Erregierre SpA (Bergamo, Italy) and glycerol palmitostearate (Precirol® ATO 5, PCR) came from Gattefossé (Cedex, France). Tween 80 (polyoxyethylene-sorbitan-monooleate), decanoic acid (≥98%), lauric acid (98%) were purchased from Sigma-Aldrich Chemie GmbH (Steinheim, Germany). Myristic acid (99%), palmitic acid (98%), stearic acid (97%), eicosanoic acid (99%) were supplied by Acros (Geel, Belgium). Hydroxypropylmethylcellulose (HPMC K100M) was obtained from Dow Chemicals (Midland, U.S.A.). Methanol (CHROMASOLV® for HPLC), *p*-toluene sulfonic acid and $NH_4H_2PO_4$ were purchased from Rielden-de Haën AG (Seelze, Germany), and isopropyl al-

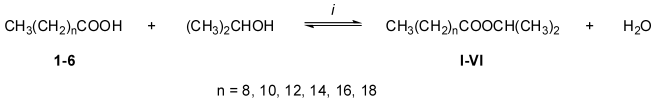

Reagents and conditions: i) *p*-Toluene sulfonic acid, 60 °C, 72 h.

Chart 1. Synthesis of the Fatty Esters I—VI

* To whom correspondence should be addressed. e-mail: vsanna@uniss.it

cohol from Carlo Erba (Milano, Italy). All other solvents and chemicals were of analytical grade.

General Melting points (mp) were determined using an electrothermal or a Köfler apparatus and are uncorrected. Infrared (IR) spectra were recorded in nujol with a Perkin-Elmer 781 IR spectrophotometer and are expressed in ν (cm^{-1}). Nuclear magnetic resonance (^{1}H-NMR) spectra were determined in $CDCl_3$ on a Varian XL-200 (200 MHz) spectrometer. Chemical shifts (δ scale) are reported in parts per million (ppm) downfield from tetramethylsilane (TMS) used as an internal standard. Electron ionization mass spectra (EI-MS) (70 eV) were recorded on a Hewlett-Packard 5989 Mass Engine Spectrometer. Elemental analyses were performed on a Perkin-Elmer 2400 instrument; all values are given as percentages, and the results were within ±0.4% of the theoretical values.

Chemical Procedure for the Synthesis of Fatty Esters (I—VI) A mixture of the appropriate fatty acid (**1**—**6**) (10 mmol) and *p*-toluene sulfonic acid (1 mmol) was dissolved in isopropyl alcohol (50 ml) and stirred for 72 h at 60 °C. Then, the solution was evaporated to dryness and extracted with ethyl acetate by using 10% (w/v) sodium hydroxide as the aqueous phase. The organic layers were dried over anhydrous sodium sulphate and evaporated under reduced pressure to give the desired isopropyl esters (I—VI) as oil or amorphous solid, which were used without further purification. Spectral and analytical data of all the synthesized title compounds are given below.

Isopropyl Decanoate (IPD, I): Yield 91.4%; colorless oil. ^{1}H-NMR ($CDCl_3$) δ: 5.09—4.91 (1H, m), 2.25 (2H, t), 1.61 (2H, t), 1.23 (6H, d), 1.42—1.16 (18H, m), 0.88 (3H, t). IR (Nujol) cm^{-1}: 1735. MS *m*/*z*: 214 (M^+). *Anal.* Calcd for $C_{13}H_{26}O_2$: C, 72.84; H, 12.23. Found: C, 72.71; H, 12.45.

Isopropyl Laurate (IPL, II): Yield 88.0%; yellow oil. ^{1}H-NMR ($CDCl_3$) δ: 5.09—4.91 (1H, m), 2.25 (2H, t), 1.61 (2H, t), 1.40—1.18 (22H, m), 0.88 (3H, t). IR (Nujol) cm^{-1}: 1735. MS *m*/*z*: 242 (M^+). *Anal.* Calcd for $C_{15}H_{30}O_2$: C, 74.32; H, 12.473. Found: C, 74.03; H, 12.41.

Isopropyl Myristate (IPM, III): Yield 93.5%; yellow oil. ^{1}H-NMR ($CDCl_3$) δ: 5.09—4.91 (1H, m), 2.25 (2H, t), 1.61 (2H, t), 1.40—1.18 (26H, m), 0.88 (3H, t). IR (Nujol) cm^{-1}: 1735. MS *m*/*z*: 270 (M^+). *Anal.* Calcd for $C_{17}H_{34}O_2$: C, 75.50; H, 12.67. Found: C, 75.59; H, 12.84.

Isopropyl Palmitate (IPP, IV): Yield 89.3%; yellow oil. ^{1}H-NMR ($CDCl_3$) δ: 5.13—4.94 (1H, m), 2.25 (2H, t), 1.61 (2H, t), 1.44—1.18 (30H, m), 0.88 (3H, t). IR (Nujol) cm^{-1}: 1735. MS *m*/*z*: 298 (M^+). *Anal.* Calcd for $C_{19}H_{38}O_2$: C, 76.45; H, 12.83. Found: C, 76.54; H, 13.09.

Isopropyl Stearate (IPS, V): Yield 94.4%; yellow oil. ^{1}H-NMR ($CDCl_3$) δ: 5.09—4.93 (1H, m), 2.29—2.02 (2H, br s), 1.68—1.55 (2H, t), 1.45—1.16 (34H, m), 0.94—0.82 (3H, br s). IR (Nujol) cm^{-1}: 1735. MS *m*/*z*: 326 (M^+). *Anal.* Calcd for $C_{21}H_{42}O_2$: C, 77.24; H, 12.96. Found: C, 76.11; H, 12.72.

Isopropyl Arachidate (IPA, VI): Yield 92.3%; white crystal. mp 53—55 °C. ^{1}H-NMR ($CDCl_3$) δ: 5.07—4.93 (1H, m), 2.29—2.02 (2H, br s), 2.25 (2H, t), 1.45—1.16 (38H, m), 0.94—0.82 (3H, br s). IR (Nujol) cm^{-1}: 1735. MS *m*/*z*: 354 (M^+). *Anal.* Calcd for $C_{23}H_{46}O_2$: C, 77.90; H, 13.07. Found: C, 77.81; H, 13.22.

Preparation of Nanoparticles ECN-loaded nanoparticles were prepared by high shear homogenization method, as previously described,[19] by using a mixture of various isopropyl fatty esters (I—VI) and PCR as the lipid phase. Their compositions are reported in Table 1.

Briefly, the oil phase consisting of PCR (3% w/w), fatty ester (2% w/w) and drug (1% w/w) was heated at 80 °C. After dispersion in a surfactant solution (Tween 80, 2.5% w/w) having the same temperature, the mixture was treated by high shear homogenization (Silverson L4R mixer, Crami, Italy), emulsifying at 6200 rpm for 5 min. The resulting nanoemulsions were rapidly cooled to room temperature to obtain nanoparticle dispersions. Each preparation was carried out in triplicate.

Freeze-Drying of Nanoparticles A weighed amount of nanoparticle aqueous dispersion was rapidly frozen below −80 °C in a deep-freezer (Dairei Co., Ltd., Tokyo, Japan) and lyophilized using a 5Pascal LIO 5P apparatus (Cinquepascal srl, Milano, Italy). The freeze-drying process was carried out at −54.5 °C under vacuum (0.909 mbar) for 8 h and then the lipid powders were collected for yields of production, encapsulation efficiency and DSC measurements.

Particle Size Determination The mean particle size and polydispersity index (PI) of nanoparticle dispersions were measured by photon correlation spectroscopy (Coulter N5, Beckman Coulter, Miami, FL, U.S.A.). The analyses were performed using the following conditions: fluid refractive index: 1.333; temperature: 20 °C; viscosity: 0.890 centipoises; fixed scattering angle of 90°; sample time: 3.0 μs; sample run time: 300 s. Before the analysis, each sample was diluted with double-distilled water to the appropriate concentration of particles and sonicated for 10 s. All measurements were done in triplicate and data were expressed as mean value±standard deviation (S.D.).

Drug Content and Yields of Production The amount of ECN entrapped in the lipid matrix was determined as follows: the freeze-dried nanoparticles (50 mg) were dissolved in methanol (10 ml) at 80 °C and then slowly cooled to room temperature to precipitate the lipid. After centrifugation (3000 rpm, 5 min), an aliquot of supernatant was diluted 100 times with methanol and analyzed by HPLC. The drug content and the encapsulation efficiency (EE) were expressed as percentage, and calculated according to the following equations:

$$\text{drug loading content (\%)} = (\text{weight of drug in nanoparticles/weight of prepared nanoparticles}) \times 100$$

$$\text{EE (\%)} = (\text{weight of drug entrapped in nanoparticles/weight of drug used for nanoparticle preparation}) \times 100$$

The percentage of production yield was calculated as the weight percentage of the final product after lyophilization, with respect to the initial total amount of solid materials used for the preparation. The results were expressed as the mean of three replicates for each batch.

HPLC Analysis HPLC analyses were carried out using a previously reported modified method.[19] The equipment consisted of a Varian Prostar 210 HPLC system that included an autosampler Varian 410 and a diode array detector (DAD) Varian 330 (Varian Deutschland GmbH, Dramstad, Germany) set to 200 nm. The chromatographic separation was performed using a spherisorb octyl 5 μm RP-C8 column (250×4.6 mm, Supelco, Milano, Italy). A mixture of methanol and 0.05 M $NH_4H_2PO_4$ (85/15, v/v) was used as the mobile phase, at a flow of 1.0 ml/min. Injection volume was 20.0 μl.

Differential Scanning Calorimetry (DSC) Thermal measurements were performed on freeze-dried particles using a DSC Q100 calorimeter (TA Instrument, New Castle, U.S.A.). The instrument was calibrated using an indium standard and the sample was analysed against a hermetic empty reference pan. The measurements were obtained at a scanning rate of 10 °C/min and performed under an Ar purge (50 ml/min). DSC analysis was carried out on ECN, on PCR, on a physical mixture of ECN–PCR–isopropyl esters (I—VI), and on drug loaded nanoparticles.

***Ex-Vivo* Permeation Experiments** After preparation, the nanoparticles were formulated into hydrogels by addition of HPMC K100M (2%, w/w), selected as gelling agent, to the nanoparticles dispersions. The mixture was stirred at room temperature at approximately 1000 rpm for 15 min. The obtained hydrogels contained a final ECN concentration of 1% w/w.

Porcine skin is a good model frequently used for human skin showing a similar penetration for topically applied compounds.[20,21] Pig ears were collected immediately after animal death from a local slaughterhouse. Hairs on both the surfaces of ears were removed using a hair clipper. The epidermis was separated by heating the skin in distilled water at 60 °C for 2 min and SC was gently peeled off. Skin samples were frozen at −20 °C in an aluminum foil until using.

For permeation studies, the frozen skin was hydrated for 30 min at 32 °C in receptor medium. The SC was cut and mounted on the bottom of a cylindrical plastic support connected to a drive shaft of the modified dissolution apparatus (Erweka DT 70, Erweka GmbH, Heusenstamm, Germany) as previously reported.[19] A methanol/water solution (70/30, v/v) (200 ml) was used as the receptor medium. Manually, 1 ml samples were taken hourly for 8 h and after 24 h, and replaced with the same volume of fresh medium. The amount of drug permeated through the SC was determined by HPLC analysis.

The permeation of ECN was investigated for 24 h and plots of the accumulated amount of ECN ($\mu g/cm^2$) against time (h) were constructed. The steady state flux, representing the absorption rate per unit area, was estimated from the slope of the linear region of the plot.

The permeability coefficient (K_p) was calculated from the following equation[22]:

$$K_p = J/C$$

where J is the flux ($\mu g/cm^2/h$) and C the concentration of ECN in the donor compartment ($\mu g/cm^3$).

Results were reported as mean±S.D. of five determinations.

Statistical Analysis All data were subjected to one-way analysis of variance (ANOVA) (Origin®, version 7.0 SR0, OriginLab Corporation, MA, U.S.A.). In all cases, individual differences between formulations were evaluated using a nonparametric *post hoc* test (Tukey's test). The differences

were considered to be statistically significant when $p<0.05$.

Results and Discussion

Synthesis of Isopropyl Fatty Esters Different methods known for the selective esterification of aliphatic carboxylic acids have been also applied to the preparation of fatty esters.[23,24] For example, these compounds can formally be prepared by reacting the corresponding fatty acid and the alcohol in different reaction conditions.[25] Although all of these methods have some degree of general applicability, most of them are associated with several drawbacks such as complex, expensive and hazardous reagents, tedious experimental procedures, and formation of undesired side products.[26] As described above, the desired fatty esters (I—VI) were obtained in high yields (88—94%) by treating the appropriate fatty acid with isopropyl alcohol in large molar excess, in the presence of a catalytic amount of *p*-toluene sulfonic acid (Chart 1). Esters were fully characterized by means of IR, NMR, mass spectrometry (EI) and elemental analysis.

Preparation and Characterization of Nanoparticles Nanoparticles based on PCR and different isopropyl fatty esters (C_{13}—C_{23}), loaded with ECN, were successfully produced by high shear homogenization method. The mean diameter and the polydispersity indexes of the prepared nanoparticles are listed in Table 1.

The results indicated that the particle mean diameter for formulations S0—S5 ranged from a minimum of 182 nm for S0 to a maximum of 283 nm for S1, independently of the isopropyl ester used.

Additionally, the size distribution processor (SDP) analysis demonstrated that the S5 formulations (containing solid lipids) were characterized by a narrow and unimodal distribution while, in the case of nanoparticles containing a solid and liquid lipid mixture, a broader particle size distribution was achieved.

The effect of different isopropyl fatty esters on drug content, encapsulation efficiency and yields of production of lipid nanoparticles were investigated and the results are reported in Table 2. The high incorporation capability of lipid nanoparticles can be ascribed to the high lipophilicity of the drug.[5] Besides, the presence of the lipid mixture (PCR and fatty ester) produced an irregular crystalline structure that promotes the accommodation of the drug molecules.[27,28] Furthermore, the yields of production obtained resulted significantly high and ranged from 80 to 98%. For all formulations, the incorporation of ECN led to similar EE values that were higher than 98%.

Differential Scanning Calorimetry To determine the degree of crystallinity of the lipid nanoparticles, a series of DSC experiments were carried out. Figure 1 shows the comparison between the DSC thermograms of ECN (pure drug), of Precirol (PCR) and of the loaded nanoparticles (S0—S5 batches), recorded from −10 to 200 °C. The DSC scan of ECN displayed a single melting peak at 165 °C, followed by an irregular exotherm as a result of the drug decomposition.[29]

The DSC curves of the loaded nanoparticles did not show a melting peak for ECN. This absence can be attributed to drug dissolution in the molten lipid when the sample was heating up. This result was confirmed by the physical mixtures of ECN–PCR–isopropyl esters, which also revealed the absence of a drug peak (data not reported).

Table 1. Mean Diameter and Polydispersity Index (PI) of Lipid Nanoparticles (Mean±S.D.)

Batch	Isopropyl ester	Mean diameter (nm)	PI
S0	IPD (I)	182.1±11.71	0.54±0.02
S1	IPL (II)	282.8±3.42	0.49±0.01
S2	IPM (III)	227.8±45.02	0.46±0.10
S3	IPP (IV)	279.7±13.14	0.39±0.04
S4	IPS (V)	232.9±22.71	0.55±0.02
S5	IPA (VI)	275.6±3.20	0.37±0.02

Table 2. Drug Content, Encapsulation Efficiency (EE), and Yield of Production of Lipid Nanoparticles (Mean±S.D.)

Batch	Drug content (w/w)	EE (%)	Yield of production (%)
S0	11.82±0.30	100.50±2.52	87.06±2.40
S1	11.91±0.06	101.24±0.49	88.24±1.18
S2	11.84±0.20	100.71±1.72	90.19±1.36
S3	11.76±0.03	99.97±0.21	80.00±2.36
S4	11.50±0.31	97.82±2.64	94.75±0.65
S5	11.50±0.11	97.81±0.90	98.04±2.71

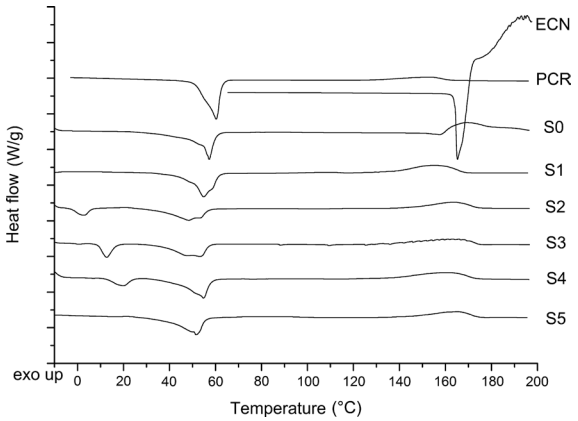

Fig. 1. DSC Thermograms of Pure Drug (ECN), Pure Precirol (PCR) and Loaded Lipid Nanoparticle Batches (S0—S5)

S0 and S1 formulations presented only the PCR melting peak at around 55°C, because the lower chain length isopropyl esters (IPD and IPL) are liquid at the tested temperatures. In the case of S2, S3 and S4 batches, the peak of fatty esters (IPM, IPP and IPS) were observed at 2, 13 and 19 °C, respectively, because these esters congealed during the DSC experiment. Moreover, these scans showed an even larger endothermic peak of PCR at 48—54 °C. According to literature,[30] the addition of a liquid lipid into the matrix determined a shift of the PCR melting point (at about 60 °C) to lower temperatures. This decrease can be attributed to the defects in the crystalline lattice due to the incorporation of liquid esters in the Precirol matrix.

On the other hand, a little increase of the melting peak with respect to pure materials for all esters was observed, thus suggesting that, during the preparation, inside the lipid nanoparticles, the segregation of the fatty esters brought to the formation of zones rich of this lipid oil.[6] Then, the formulation S5 was characterized by a larger endothermic peak at around 50 °C associated to the simultaneous fusion of the

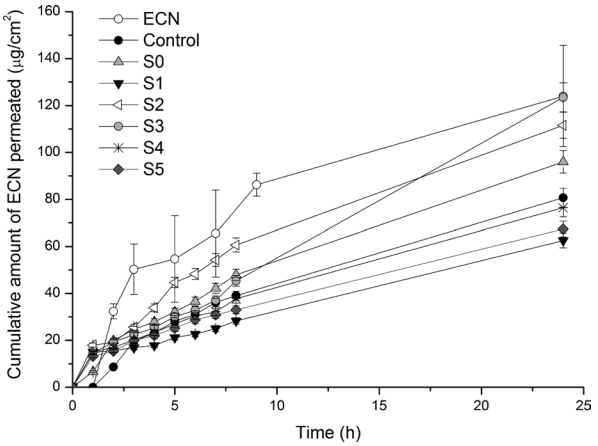

Fig. 2. *Ex Vivo* Permeation Profiles of ECN from Gels Containing Free Drug (ECN), Drug Loaded Nanoparticles Based on Precirol ATO (Control), and Nanoparticles Including Isopropyl Fatty Esters Having Different Chain Length and Precirol ATO (S0—S5) as Lipid Phase (Mean±S.D., $n=5$)

The data of ECN and Control gels are reported from ref. 19.

ester IPA (melting point=53 °C) and PCR.

***Ex-Vivo* Permeation Studies** The effect the chain length of isopropyl esters incorporated into nanoparticles on *ex vivo* skin permeation of ECN through porcine SC was investigated. The plot of the cumulative amounts of ECN permeated from gels as a function of time is depicted in Fig. 2.

As previously reported,[19] the gel containing ECN not incorporated in nanoparticles (indicated as ECN gel) showed an irregular permeation profile and a lag time of 60 min. The drug encapsulation into PCR nanoparticles without isopropyl fatty esters (Control gel) decreased the permeation with a lag time of 1.19 h, but also reduced the variability in the release behaviour of the free drug.

Drug profiles of all formulations containing fatty esters resulted similar and typically characterized by a rapid permeation rate with no lag time. Statistical analysis showed that the drug permeated after 24 h was significantly higher ($p<0.05$) for ECN gel (124.18±0.12 μg/cm^2), followed by S3 gel (123.52±1.42 μg/cm^2), S2 gel (111.62±2.79 μg/cm^2), S0 gel (96.01±3.40 μg/cm^2), Control gel (80.72±4.06 μg/cm^2) and S4 gel (76.45±0.65 μg/cm^2). On the other hand, no significant differences are found from the comparison between S1 and S5 gels ($p>0.05$) that released the lowest amount of ECN (62.55±3.14 μg/cm^2 and 67.39±3.42 μg/cm^2, for S1 and S5, respectively).

Furthermore, from the analysis of permeation data reported in Table 3, a non direct relationship between the chain length of fatty ester and the flux values of ECN was observed.

In particular, for S0 gel, containing the IPC ester with the shortest chain, the flux of ECN resulted of 3.46 μg/cm^2/h. An increase of ester chain length from 13 to 15 carbon atoms (S1 gel) determined a significant ($p>0.05$) decrease of ECN skin permeability (2.15 μg/cm^2/h). Nevertheless, when the chain length increased to 17 and 19 carbons the highest flux of ECN were obtained (4.08 and 4.79 μg/cm^2/h for S2 and S3 gels, respectively). These values resulted almost equivalent to ECN gel containing only the pure drug (4.36±0.48 μg/cm^2/h) and were significantly higher ($p<0.05$) with respect to Control gel (3.66±0.13 μg/cm^2).

Table 3. Permeation Data of ECN Delivered from Gels through Porcine Skin (Mean±S.D., $n=5$)

Gel	J (μg/cm^2/h)	$K_p\times10^{-5}$ (cm/s)
ECN	4.36±0.48[a)]	12.12±0.71[a)]
Control	3.66±0.13[a)]	10.06±0.36[a)]
S0	3.46±0.11	9.56±0.20
S1	2.15±0.22	5.97±0.60
S2	4.08±0.19	11.33±0.05
S3	4.79±0.14	13.30±0.40
S4	2.49±0.07	7.15±0.18
S5	2.32±0.09	6.45±0.35

a) Data reported from ref. 19.

Then again, S4 and S5 formulations, containing the esters with the longest chains (21 and 23 carbon atoms, respectively) were characterized by the lowest flux values that resulted comparable to that of S1 gel. Moreover, an analogous parabolic correlation between the K_p values and the incorporated ester chain length was observed, with a maximum for S2 and S3 gels containing IPM and IPP esters with 17 and 19 carbons, respectively. This result is in agreement with previous studies, which reported the use of different fatty acids in propylene glycol solution to improve the *p*-aminobenzoic acid permeation through human SC.[12]

As also suggested by Kadir *et al.*[31] the enhancement ability of fatty acids has been explained as a result of an optimum balance between the "pull" and "push" forces; the first effect is related to the excess of free energy of the drug in the donor phase containing the fatty acids, while the second force originated from the permeability coefficient of the pure fatty acid across the skin. The relationship between fatty acids and fatty esters can be correlated with the mechanism of action of these compounds due to an intercalation into the structured lipids of the SC and the disturbance of the lipid packing order.

On the other hand, in this study the effect of fatty acid esters on ECN permeation obtained cannot be explained only as result of a single phenomenon, but as a complex combination of different factors. In fact, it is essential to consider also the distribution of liquid lipid (fatty ester) in the nanoparticles matrix, the preferential solubility of lipophilic drug in the lipid phase (PCR or fatty ester), and finally the interaction of the fatty ester to the skin lipid. Additionally, it is of major interest to elucidate in more detail the mode of action of the prepared nanoparticles on permeation of ECN across porcine SC. Work is ongoing in this direction to build on the above-mentioned results, and to perform further studies in this field.

Conclusions

In this work a simple, highly efficient, and inexpensive general method for the preparation of long chain fatty acid esters was developed. Next, a set of these esters was successfully incorporated into lipid nanoparticles containing as a lipid phase PCR by the high shear homogenization technique. Therefore, the influence of their chain length on permeation enhancement ability of the nanoparticulate systems was evaluated. In particular, among the investigated nanoparticles, the formulations containing isopropyl myristate (III) and isopropyl palmitate (IV) esters resulted more effective for augmenting skin permeation of ECN and may become

promising systems for its topical delivery.

Acknowledgments The authors thank the Dipartimento di Scienze del Farmaco of the University of Sassari for facilities. VS is grateful to Master & Back Program of Regione Autonoma della Sardegna.

References

1) Santos Maia C., Mehnert W., Schaller M., Korting H. C., Gysler A., Haberland A., Schafer-Korting M., *J. Drug Target*, **10**, 489—495 (2002).
2) Sivaramakrishnan R., Nakamura C., Mehnert W., Korting H. C., Kramer K. D., Schafer-Korting M., *J. Controlled Release*, **97**, 493—502 (2004).
3) Lombardi Borgia S., Regehly M., Sivaramakrishnan R., Mehnert W., Korting H. C., Danker K., Roder B., Kramer K. D., Schafer-Korting M., *J. Controlled Release*, **110**, 151—163 (2005).
4) Muller R. H., Radtke M., Wissing S. A., *Adv. Drug Deliv. Rev.*, **54**, S131—155 (2002).
5) Souto E. B., Wissing S. A., Barbosa C. M., Muller R. H., *Int. J. Pharm.*, **278**, 71—77 (2004).
6) Castelli F., Puglia C., Sarpietro M. G., Rizza L., Bonina F., *Int. J. Pharm.*, **304**, 231—238 (2005).
7) Souto E. B., Wissing S. A., Barbosa C. M., Muller R. H., *Eur. J. Pharm. Biopharm.*, **58**, 83—90 (2004).
8) Benson H. A. E., *Curr. Drug Deliv.*, **2**, 23—33 (2005).
9) Mehnert W., Mader K., *Adv. Drug Deliv. Rev.*, **47**, 165—196 (2001).
10) Hu F. Q., Jiang S. P., Du Y. Z., Yuan H., Ye Y. Q., Zeng S., *Coll. Surf. B: Biointerfaces*, **45**, 167—173 (2005).
11) Hu F. Q., Jiang S. P., Du Y. Z., Yuan H., Ye Y. Q., Zeng S., *Int. J. Pharm.*, **314**, 83—89 (2006).
12) Tanojo H., Bouwstra J. A., Junginger H. E., Bodde H. E., *Pharm. Res.*, **14**, 42—49 (1997).
13) Fujii M., Hori N., Shiozawa K., Wakabayashi K., Kawahara E., Matsumoto M., *Int. J. Pharm.*, **205**, 117—125 (2000).
14) Santoyo S., Ygartua P., *Eur. J. Pharm. Biopharm.*, **50**, 245—250 (2000).
15) Trommer H., Neubert R. H., *Skin Pharmacol. Physiol.*, **19**, 106—121 (2006).
16) Elyan B. M., Sidhom M. B., Plakogiannis F. M., *J. Pharm. Sci.*, **85**, 101—105 (1996).
17) Takeuchi Y., Yamaoka Y., Fukushima S., Miyawaki K., Taguchi K., Yasuka H., Kishimoto S., Suzuki M., *Biol. Pharm. Bull.*, **21**, 484—491 (1998).
18) Bhatia K. S., Singh J., *J. Pharm. Sci.*, **87**, 462—469 (1998).
19) Sanna V., Gavini E., Cossu M., Rassu G., Giunchedi P., *J. Pharm. Pharmacol.*, **59**, 1057—1064 (2007).
20) Simon G. A., Maibach H. I., *Skin Pharmacol. Appl. Skin Physiol.*, **13**, 229—234 (2000).
21) Benech-Kieffer F., Wegrich P., Schwarzenbach R., Klecak G., Weber T., Leclaire J., Schaefer H., *Skin Pharmacol. Appl. Skin Physiol.*, **13**, 324—335 (2000).
22) Vaddi H. K., Ho P. C., Chan Y. W., Chan S. W., *J. Controlled Release*, **81**, 121—133 (2002).
23) Parrish J. P., Dueno E. E., Kim S.-I., Jung K. W., *Synth. Comm.*, **30**, 2687—2700 (2000).
24) Vandevoorde S., Tsuboi K., Ueda N., Jonsson K. O., Fowler C. J., Lambert D. M., *J. Med. Chem.*. **46**, 4373—4376 (2003).
25) Awang R., Basri M., Sallah A. B., *J. Am. Oil Chem. Soc.*, **77**, 609—612 (2000).
26) Sekeroglu G., Fadiloglu S., Ibanoglu E., *Turkish J. Eng. Env. Sci.*, **28**, 241—247 (2004).
27) Jenning V., Gohla S. H., *J. Microencapsul.*, **18**, 149—158 (2001).
28) Jenning V., Thunemann A. F., Gohla S. H., *Int. J. Pharm.*, **199**, 167—177 (2000).
29) Godefroi E. F., Heeres J., Van Cutsem J., Janssen P. A., *J. Med. Chem.*, **12**, 784—791 (1969).
30) Fang J. Y., Fang C. L., Liu C. H., Su Y. H., *Eur. J. Pharm. Biopharm.*, **70**, 633—640 (2008).
31) Kadir R., Stempler D., Liron Z., Cohen S., *J. Pharm. Sci.*, **76**, 774—779 (1987).